# Anion Permeation in Human ClC-4 Channels

Simon Hebeisen,* Hannelore Heidtmann,* Diego Cosmelli,[†] Carlos Gonzalez,[†] Barbara Poser,*
Ramon Latorre,[†‡] Osvaldo Alvarez,[†‡] and Christoph Fahlke*[†]

*RWTH Aachen, Institute of Physiology, Aachen, Germany; [†]Centro de Estudios Cientificos, Valdivia, Chile; and
[‡]Departamento de Biologia, Facultad de Ciencias, Universidad de Chile, Santiago, Chile

ABSTRACT   ClC-4 and ClC-5 are mammalian ClC isoforms with unique ion conduction and gating properties. Macroscopic current recordings in heterologous expression systems revealed very small currents at negative potentials, whereas a substantially larger instantaneous current amplitude and a subsequent activation were observed upon depolarization. Neither the functional basis nor the physiological impact of these channel features are currently understood. Here, we used whole-cell recordings to study pore properties of human ClC-4 channels heterologously expressed in tsA201 or HEK293 cells. Variance analysis demonstrated that the prominent rectification of the instantaneous macroscopic current amplitude is due to a voltage-dependent unitary current conductance. The single channel amplitudes are very small, i.e., $0.10 \pm 0.02$ pA at $+140$ mV for external $Cl^-$ and internal $I^-$. Conductivity and permeability sequences were determined for various external and internal anions, and both values increase for anions with lower dehydration energies. ClC-4 exhibits pore properties that are distinct from other ClC isoforms. These differences can be explained by assuming differences in the size of the pore narrowing and the electrostatic potentials within the ion conduction pathways.

## INTRODUCTION

ClC-type voltage-gated $Cl^-$ channels form a large gene family encoding for anion channels. Nine human isoforms (ClC-1 to ClC-7, ClC-Ka, and ClC-Kb) are expressed in various tissues and fulfill many physiological functions. ClC-1 is the major muscle chloride channel responsible for the regulation of muscle excitability (Koch et al., 1992; George et al., 1993), ClC-Kb is the predominant basolateral anion channel in the thick ascending limb of Henle (Simon et al., 1997), and ClC-3, ClC-5, and ClC-7 are necessary for the pH adjustment of several cell compartments (Lloyd et al., 1996; Stobrawa et al.; 2001; Kornak et al., 2001).

Whereas ClC-0 and ClC-1 have been studied in great detail during the last years, the properties of other isoforms are still insufficiently understood. ClC-4 (van Slegtenhorst et al., 1994; Jentsch et al., 1995) is highly homologous to ClC-3 and ClC-5, and forms with them a distinct branch of the ClC family. It is expressed in the apical brush border membrane of the intestine of mice, rats, and humans (Mohammad-Panah et al., 2001) suggesting that this ClC isoform may operate in parallel with CFTR in epithelial chloride secretion. ClC-4 expression was also demonstrated in brain, heart, and skeletal muscle, but so far no functional role has been attributed in these tissues. In various expression systems ClC-4 exhibits characteristic and well reproducible features that are similar to those observed for ClC-5. In *Xenopus* oocytes as well as in mammalian cells,

ClC-4 and ClC-5 mediate a chloride current with marked outward rectification and activation gating at positive potentials (Mindell et al., 1998; Friedrich et al., 1999; Vanoye and George, 2002).

During the last years we have developed a model of anion selectivity for the human muscle ClC isoform, ClC-1 (Fahlke et al., 1997a,b,c; Fahlke, 2001). The unique pore properties of human ClC-4 provide a test whether this model also applies to other ClC isoforms and a tool to identify the functional basis of different pore properties within the ClC family. Although relative anion conductivities of ClC-4 have been published (Friedrich et al., 1999; Kawasaki et al., 1999; Vanoye and George, 2002), a detailed analysis of the permeation mechanisms of ClC-4 is still missing. In this study, we examined permeation properties of ClC-4 in mammalian cells with the patch clamp technique and found that anion permeation through this ClC isoform is different from others ClC isoforms and from other anion channel families.

## MATERIALS AND METHODS

### ClC-4 expression in tsA201 and in HEK293 cells

We purchased ClC-4 as an EST clone (I.M.A.G.E. ID 712030). The coding region of ClC-4 was then subcloned into a pRcCMV vector (Invitrogen, Carlsbad, CA) after modifying the original construct by PCR techniques to produce an N-terminal *Not*I restriction site and a C-terminal *Xba*I site. We sequenced regions modified by PCR completely to exclude polymerase errors. Two independent recombinants were examined that exhibited indistinguishable functional properties. Transient transfection of tsA201 using the $Ca_3(PO_4)_2$ technique was performed as previously described (Fahlke et al., 1997a), and cells were typically examined two days after transient transfection. To identify cells with a high probability of expressing recombinant ion channels, cells were cotransfected with a plasmid encoding the CD8 antigen and incubated 5 min before use with polystyrene microbeads precoated with anti-CD8 antibody (Dynabeads M-450 CD 8,

Address reprint requests to Christoph Fahlke, Institut für Physiologie, RWTH Aachen, Pauwelsstr. 30, D-52074 Aachen, Germany. Tel.: 49-241-80-88810; Fax: 49-241-80-82434; E-mail: chfahlke@physiology.rwth-aachen.de.

Dynal, Great Neck, NY; see also Jurman et al., 1994). Only cells decorated with microbeads were used for electrophysiological recordings. By adjusting the CD8/hClC-4 cDNA ratio we optimized our conditions so that essentially every cell with beads exhibited a current component with characteristic properties shown in Fig. 1.

Oligoclonal cell lines were obtained by selection for resistance to the aminoglycoside antibiotics Geneticin (G418, Boehringer Mannheim, Germany). 24 h after transfection HEK 293 cells were incubated in medium supplemented with G418 (0.9 mg/ml). After 23 days, G418-resistant foci were picked, plated in individual flasks, and electrophysiologically tested after growing periods of three to six days. Cells lines in which more than three consecutively tested cells did not show current amplitudes >200 pA at +150 mV, were classified as negative. Of the cell lines four were positive, and two of them were grown in culture for 3 months. Stably transfected cells showed a late current amplitude of $1.03 \pm 0.1$ nA ($n = 26$) at +150 mV under standard internal and external solutions. Current recordings in transiently transfected tsA201 cells and stably transfected HEK293 cells revealed indistinguishable results.

## Whole-cell recordings

Standard whole-cell patch clamp recordings (Hamill et al., 1981) were performed using an Axopatch 200B (Axon Instruments, Union City, CA), an EPC-8 or an EPC-9 (HEKA Electronics, Lambrecht, Germany) amplifier. Borosilicate pipettes were pulled with resistances of 0.8–2.2 M$\Omega$. Cell capacitances ($16 \pm 1$ pF, $n = 7$) and charging time constants ($50 \pm 4 \mu s$, $n = 7$) were determined using current responses to a 0.5 ms voltage step from 0 mV to 5 mV. More than 80% of the series resistance was compensated by an analog procedure. The calculated voltage error due to series resistance was always <5 mV. Currents were digitized with various sampling rates using a Digidata AD/DA converter (Axon Instruments, Union City, CA) or an ITC-16 converter (HEKA Electronics, Lambrecht, Germany) after analog filtering with less than one-third of the sampling frequency. Cells were clamped to 0 mV for at least 3 s between two test sweeps.

In the majority of our recordings, we observed a time-dependent decrease (rundown) of the current amplitudes at positive potentials as described recently (Vanoye and George, 2002). All data presented in this paper were collected after the rundown had reached steady-state conditions, i.e., when three consecutive recordings exhibited identical late and instantaneous current amplitudes. During longer lasting experiments, cells were tested repeatedly in standard external solution to ensure that no additional rundown had occurred. In contrast to earlier reports (Vanoye and George, 2002), we never observed a complete current rundown, i.e., under steady-state conditions all positive cells exhibited anion currents with a typical rectification and anion selectivity. Rundown was associated with a reduction of the relative amplitude of the activating current component. Most likely for this reason, there was a certain variability in the relative amplitude of the activating current that was not further investigated.

The composition of the standard solutions were: extracellular (in mM) 140 NaCl, 4 KCl, 2 CaCl$_2$, 1 MgCl$_2$, 5 HEPES, pH 7.4, intracellular (in mM) 120 NaCl, 2 MgCl$_2$, 5 EGTA, 10 HEPES, pH 7.4. For the determination of anion permeability and conductivity ratios for external anions, cells were moved into the stream of solutions containing various sodium salts (in mM) 150 NaX, 5 HEPES, pH 7.4; X denotes Cl$^-$, Br$^-$, I$^-$, NO$_3^-$, N$_3^-$, SCN$^-$, F$^-$, HCO$_3^-$, CH$_3$COO$^-$, CH$_3$SO$_3^-$, or glutamate$^-$. For experiments with distinct internal anions, cells were perfused with a solution containing (in mM) 123 NaX, 5 EGTA, 10 HEPES, pH 7.4; X$^-$ denotes Cl$^-$, I$^-$, NO$_3^-$, SCN$^-$, F$^-$, HCO$_3^-$, and glutamate$^-$. For experiments in which the internal or external SCN$^-$ or I$^-$ concentration was altered, the internal solution contained (in mM): $(123 - X)$ Na-glutamate, X NaI or NaSCN, 5 EGTA, 10 HEPES, pH 7.4. The external solution contained (in mM): $(150 - X)$ Na-glutamate, X NaI or X NaSCN, 5 HEPES, pH 7.4. For all these experiments, we used an external and/or internal agar salt bridge to connect the Ag/AgCl electrode, made from a plastic tubing filled with 3 M KCl in 0.3% agar. Offset potentials determined at the end of each experiment and junction potentials either calculated using the JPCalc software (Dr. P. Barry, University of South Wales, Sydney, Australia; see also Barry, 1994) or directly measured (Neher, 1992) were used to correct results.

## Data analysis

Data were analyzed with a combination of pClamp (Axon Instruments, Union City, CA) and SigmaPlot (Jandel Scientific, San Rafael, CA, USA) programs. All summary data are shown as mean $\pm$ SE.

Instantaneous current amplitudes were calculated by extrapolating the activation time course with a monoexponential function to the moment of the voltage step. For normalized current-voltage relationships in various external anions (Fig. 4), instantaneous current amplitudes were determined after a 200 ms prepulse to +75 mV. Current amplitudes, determined in different external anion compositions were normalized to the amplitude measured from the same cell at +125 mV in external Cl$^-$, and averaged. To compare current amplitudes with different internal solutions, absolute current amplitudes obtained from several cells perfused with the same internal solution were averaged (Fig. 5).

Because of the pronounced bidirectional rectification of ClC-4 channels, the macroscopic conductance of cells expressing ClC-4 at the reversal potential was quite small. Reversal potentials of cells expressing ClC-4 were only used for further analysis when the cell exhibited a whole-cell conductance that was at least three times larger than the mean value for untransfected cells under identical conditions. Permeability ratios were
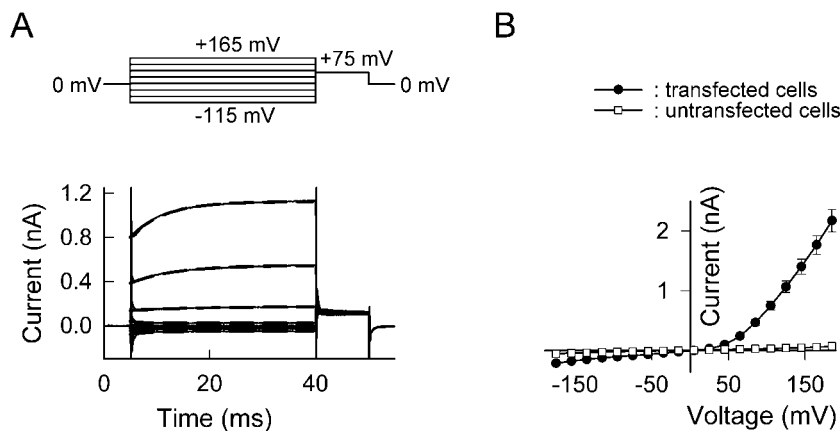


FIGURE 1 Current records from ClC-4 channels expressed in HEK293 cells (*A*) Whole-cell current recordings from a HEK293 cell stably expressing ClC-4. Cells were held at 0 mV, and voltage steps were applied to potentials between −115 and +165 mV, each followed by a fixed +75 mV step. The internal and the external solution had the standard composition. Solid lines represent original data, dashed lines monoexponential fits. (*B*) Voltage-dependence of the mean current amplitude mean $\pm$ SE from transfected (●, $n = 21$) and from untransfected (□, $n = 12$) HEK 293 cells. For transfected cells, the instantaneous current amplitudes determined by extrapolating the fitted activation time course back to the time of the voltage step was shown. Untransfected cells did not exhibit time-dependent changes of the current amplitude did; we therefore simply determined the current amplitude 2 ms after the voltage step.

**TABLE 1 Anion permeability coefficients for external anions**

| Anion | Reversal potential (mV) | $P_x/P_{Cl}$ | N |
|---|---|---|---|
| Cl | | 1 | |
| Br | $+3.0 \pm 0.6$ | $0.7 \pm 0.02$ | 3 |
| I | $-6.8 \pm 0.7$ | $1.1 \pm 0.03$ | 9 |
| F | $+4.0 \pm 0.8$ | $0.7 \pm 0.02$ | 7 |
| $NO_3$ | $-11.3 \pm 0.6$ | $1.3 \pm 0.03$ | 6 |
| $HCO_3$ | $+18.9 \pm 0.7$ | $0.4 \pm 0.09$ | 12 |
| $N_3$ | $-20.5 \pm 1.3$ | $1.9 \pm 0.09$ | 8 |
| $CH_3COO$ | $+24.8 \pm 1.5$ | $0.3 \pm 0.02$ | 3 |
| SCN | $-36.0 \pm 2.9$ | $3.4 \pm 0.40$ | 4 |
| $CH_3SO_3$ | $+18.8 \pm 4.4$ | $0.5 \pm 0.08$ | 3 |
| Glutamate | $+34.0 \pm 3.8$ | $0.3 \pm 0.04$ | 3 |

**TABLE 2 Anion permeability coefficients for internal anions**

| Anion | Reversal potential (mV) | $P_x/P_{Cl}$ | N |
|---|---|---|---|
| Cl | | 1 | |
| F | $-7.5 \pm 0.6$ | $0.9 \pm 0.1$ | 5 |
| $NO_3$ | $+11.7 \pm 2.3$ | $1.9 \pm 0.1$ | 8 |
| I | $+17.7 \pm 1.5$ | $2.4 \pm 0.1$ | 9 |
| $HCO_3$ | $+14.2 \pm 0.3$ | $0.7 \pm 0.01$ | 10 |
| SCN | $+30.2 \pm 1.7$ | $3.9 \pm 0.3$ | 7 |
| Glutamate | $-64.6 \pm 2.7$ | $0.1 \pm 0.01$ | 6 |

calculated from reversal potential measurements under biionic conditions using the Goldman-Hodgkin-Katz equation as described (Fahlke et al., 1997a; see also Tables 1 and 2, this article).

## Noise analysis

Nonstationary noise analysis was performed using an EPC-9 amplifier (HEKA Electronics, Lambrecht, Germany) equipped with a 16 bit AD/DA converter. Currents were filtered at 10 kHz and digitized with a sampling rate of 50 kHz. For all experiments, the analysis was repeated after digital filtering at 4 kHz, 2 kHz, and 500 Hz without differences in outcome. A series of 300 records were recorded by pulsing to a certain voltage from the holding potential of 0 mV. Pairs of subsequent records were then subtracted using the PulseTools software (HEKA Electronics, Lambrecht, Germany) to compute the experimental nonstationary ensemble variance (Heinemann and Conti, 1992). The variance points were sorted into evenly-spaced (10 pA) current bins. The statistical errors caused by averaging were superimposed as error bars.

The calculated variance $\sigma^2$ was plotted versus the corresponding current amplitude obtained in two distinct types of experiments. For the experiments shown in Fig. 2, the nonstationary noise measured 1 ms after the voltage steps was determined for various voltages and then plotted versus the mean current amplitudes determined at the same time. As Lorentzian noise depends on the number of channels ($N$), the unitary current amplitude ($i$), and the absolute open probability ($p$), the measured variance will be equal to

$$\sigma^2(V) = Ni^2(V)p(V)(1 - p(V)) + \sigma_0^2, \qquad (1)$$

with $\sigma_0^2$ being the background noise.

In this experiment, the unitary current amplitude is not constant and substitution of

$$i(V) = \frac{I(V)}{Np(V)} \qquad (2)$$

into Eq. 1 yields:

$$\sigma^2 = \frac{I^2(V)}{N}\left(\frac{1}{p(V)} - 1\right) + \sigma_0^2. \qquad (3)$$

For further analysis the background noise was determined as the variance at zero current and subtracted. Eq. 3 can then be transformed to Eq. 4:

$$\sigma_{app} = \sqrt{\sigma^2 - \sigma_0^2} = I(V)\sqrt{\frac{(1/p(V)) - 1}{N}}. \qquad (4)$$

To simulate the current-noise relationship for a channel with constant unitary conductance that exhibits an isochronal current rectification due to voltage-dependent changes of the open probability (Fig. 2 *D*) the following procedure was used. Assuming a certain absolute isochronal open

probability at $+175$ mV ($p_{iso}(+175 \text{ mV}) = 0.1$ or $p_{iso}(+175 \text{ mV}) = 0.7$), the unitary current amplitude at $+175$ mV and the number of channels per cell were calculated using the experimentally determined isochronal current amplitude and variance. Next, assuming a constant unitary conductance, single channel current amplitudes for voltages between $-100$ mV and $+150$ mV and the open probabilities necessary to account for the observed macroscopic current amplitude were computed. The corresponding variance was then calculated for each potential using $\sigma^2(V) = Ni^2(V) p(V) (1 - p(V))$ and plotted versus the experimentally determined current amplitude.

To determine the single channel amplitude at a certain potential, variances determined at various time periods larger than 0.5 ms after a voltage step from 0 mV to this potential were plotted versus the corresponding mean current amplitude (Fig. 3). Under these conditions, the unitary current amplitude and the number of channels is constant, whereas the open probability changes with time:

$$\sigma^2(t) = Ni^2p(t)(1 - p(t)) + \sigma_0^2. \qquad (5)$$

Substitution of

$$p(t) = \frac{I(t)}{Ni} \qquad (6)$$

leads to

$$\sigma^2 = iI(t) - \frac{I^2(t)}{N} + \sigma_0^2, \qquad (7)$$

where $i$ is the single channel current amplitude and $N$ the number of channels. These values can be obtained by parabolar fits to plots of the variance versus the current amplitude (Fig. 3).
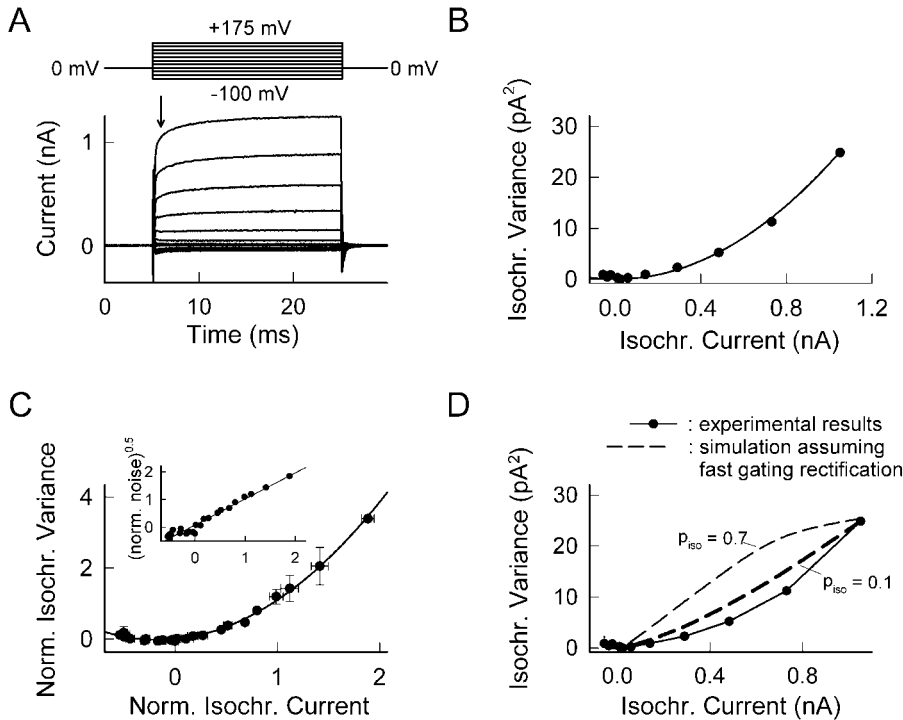
Due to the small single channel amplitude, the variance of ClC-4 currents is quite small. Thus, voltage-dependent alterations of the background noise could cause artifacts in the noise analysis. We checked for a voltage-dependent background noise using two experimental approaches. Firstly, fits with Eq. 7 were used to determine the background noise at $+100$ mV, $+120$ mV, $+140$ mV, and $+160$ mV. These values were compared to the background noise measured at the current reversal potential without observing any indication for a voltage-dependence of the background noise. Secondly, we determined the voltage-dependence of the noise in untransfected cells over a broad voltage range (between $-150$ mV and $+175$ mV). The so-obtained background noise amplitudes were at all potentials less than 10% of the noise amplitude in cells expressing ClC-4.

## Simulations of noise-current relationships

Single channel responses to voltage steps were simulated using the Noise Simulation program (www.cecs.cl; also see Alvarez et al., 2002). Average current amplitudes and variances were calculated from 300 simulated records, plotted against each other and fitted to Eq. 7.

## Permeation model simulation

We used a sequential state model with three binding sites to fit the voltage-

FIGURE 2   Variance analysis of the instantaneous current amplitude measured in mammalian cells expressing hClC-4 channels at various test potentials in standard external and internal solutions. (A) Whole-cell current recordings from a HEK293 cell stably expressing ClC-4. Cells were held at 0 mV, and voltage steps were applied to potentials between −100 and +175 mV. The internal and the external solution had the standard composition. (B) Plot of the isochronal variance versus the isochronal current amplitude obtained at potentials between −100 mV and +175 mV from a single cell. For each potential, mean current amplitude and current variance were determined at the time marked by the arrow in A. The solid line represents a fit to the function: $\sigma^2 = a \times I^2$. (C) Averaged plot of the isochronal variance versus the isochronal current amplitude from seven cells. For each cell the current amplitudes as well as the variance were normalized to the respective values at +125 mV. The solid line represents a fit to the function: $\sigma^2 = a \times I^2$. (Insert) Plot of the square root of the mean variance versus the mean isochronal current amplitude. The solid line rep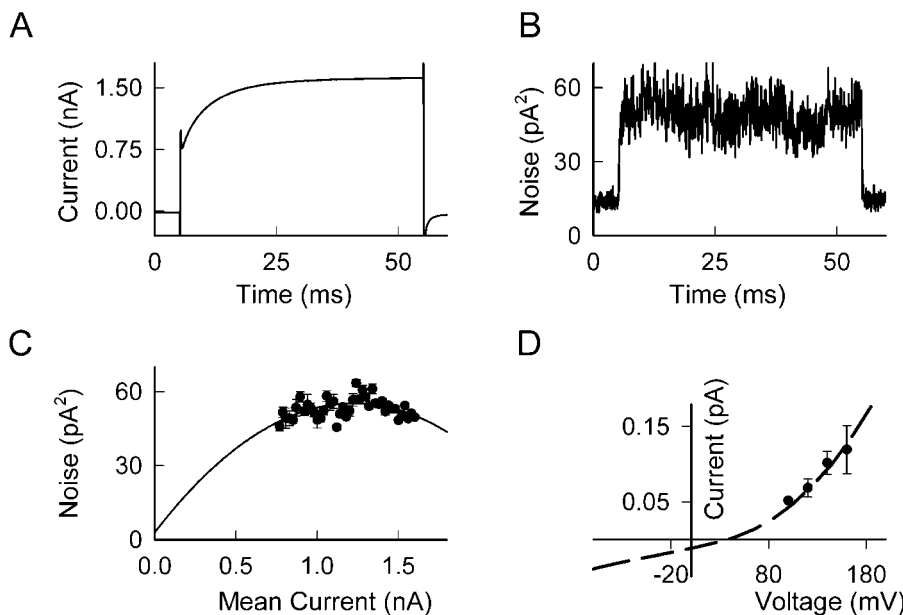resents a linear regression to the experimental data. (D) Comparison of the predicted isochronal variance-mean current plot for channels that exhibit a constant unitary conductance and macroscopic rectification because of changes of the absolute open probability (dashed lines) with the experimental results shown in B (●, solid line). Simulations were performed for an isochronal absolute open probability at +175 mV of 0.1 (thick line) and 0.7 (thin line).

dependence of unitary current amplitudes for ClC-1 and ClC-4 under two distinct external solutions: standard external solution, and a solution in which the NaCl was equimolarly substituted with NaNO₃. For ClC-4, the voltage-dependences of the instantaneous current amplitudes shown in Figs. 4 and 5 were normalized to the unitary current amplitudes determined by nonstationary noise analysis (Fig. 3). For ClC-1, instantaneous current amplitudes determined by whole-cell recordings on cells stably expressing

ClC-1 were normalized to the single channel amplitude determined by variance analysis (Rosenbohm et al., 1999). A simplex routine (kindly provided by Dr. G. Droogman, Laboratorium voor Fysiologie, KU Leuven, Belgium) was used to fit the rate constants to the data points. Following the suggestion of Andersen (1999), the properties of this model were expressed graphically with a reduced rate constant representation (see Fig. 9) using $ff = 6 \times 10^{12}$ s$^{-1}$.



FIGURE 3   Variance analysis for ClC-4 channels. The intracellular solution contained (in mM): 123 NaI, 5 EGTA, 10 HEPES, pH 7.4; the external solution had the standard composition. (A) Mean current trace obtained from 300 traces. The cell was held at 0 mV and a test step to +140 mV was applied (B) Time course of the variance. (C) Variance versus current fitted to the function $\sigma^2 = iI(t) - I(t)^2/N + \sigma_o^2$ (solid line). (D) Voltage-dependence of the unitary current amplitudes for four different test potentials (●). The dashed line represents the current-voltage relationship of the instantaneous macroscopic current from eight cells measured under identical conditions scaled down to superimpose on the single channel currents.
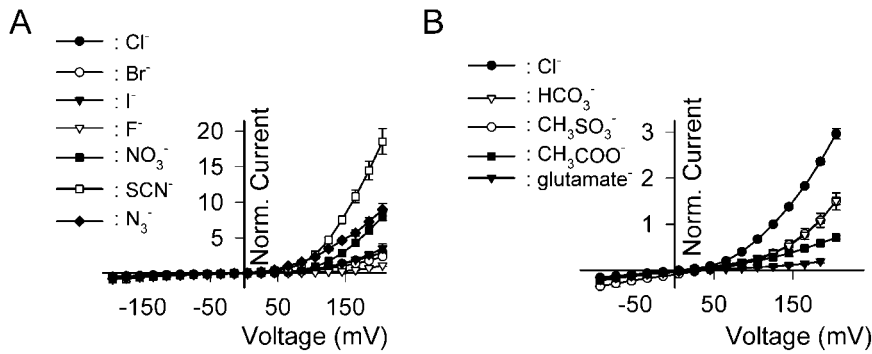
A



B



FIGURE 4 Instantaneous current amplitudes in various external solutions. (*A*) Voltage-dependence of instantaneous current amplitudes determined after a 200 ms prepulse to +75 mV for different anion compositions. Current amplitudes were measured in an external solution containing (in mM): 150 NaX, 5 HEPES, pH 7.4; $X^-$ denotes $Br^-$, $I^-$, $SCN^-$, $NO_3^-$, $F^-$, or $N_3^-$. Values are normalized to the current amplitude measured at +125 mV in the $Cl^-$-containing external solution. (*B*) Voltage-dependence of instantaneous current amplitudes determined after a 200 ms prepulse to +75 mV for additional external anions, such as methane sulfonate ($CH_3SO_3$), glutamate, $HCO_3^-$, or $CH_3COO^-$. Mean $\pm$ SE from at least three tsA201 cells.

## RESULTS

### Heterologous expression of ClC-4 channels

Fig. 1 shows representative whole-cell recordings from a HEK293 cell stably expressing ClC-4 (Fig. 1 *A*). The cell was held at 0 mV and pulses between −115 mV and +165 mV in 40 mV intervals were applied, each followed by a fixed test pulse to +75 mV. At potentials positive to +45 mV, the current amplitude increased in a time-dependent manner due to a voltage-dependent gating. Activation gating could be fit with a single exponential ($\tau = 2.4 \pm 0.2$ ms, $n = 9$). The instantaneous current amplitudes determined by extrapolating current activation back to the moment of the voltage step were distinct from zero (Fig. 1 *A*) and displayed a marked rectification at positive potentials (Fig. 1, *A* and *B*). The instantaneous conductance had a minimum value ~0 mV and again increased with more negative potentials (Fig. 1 *B*) causing a bidirectionally rectifying instantaneous current-voltage relationship.

Fig. 1 *B* shows mean instantaneous current amplitudes from cells expressing hClC-4 (●, $n = 21$) and from untransfected cells (□, $n = 12$). Untransfected cells displayed only a negligible endogenous anion current component that was distinct from current amplitudes measured in transfected cells at negative as well as at positive voltages. We tested a large number of untransfected tsA201 and HEK293 cells and never recorded currents with characteristics similar to those observed in transfected cells.

### Rectification of human ClC-4 channels

The very pronounced rectification of the instantaneous current amplitude is a characteristic feature of ClC-4 currents (Fig. 1). At negative voltages, current amplitudes are very small and a prominent macroscopic conductance can only be observed at positive potential. At first glance this behavior appears quite similar to macroscopic current recordings from voltage-dependent channels that are closed at negative potentials and exhibit a fast activation gating upon voltage steps in the positive direction. Rectification of ClC-4 has therefore often been interpreted as the result of a characteristic activation gating, i.e., it was assumed that ClC-4 channels are closed at negative potentials and voltages ~0 mV and open only at very pronounced depolarizations. However, this suggestion has not been critically tested; i.e., the alternative mechanism, that ClC-4 channels are open over the whole voltage range and that the macroscopic rectification is caused by a voltage-dependent unitary channel conductance, has never been excluded.

Instantaneous rectification was also observed in macroscopic recordings using voltage clamp techniques with faster clamp speed. In cut-open oocyte voltage clamp recordings using intra- and extracellular $Cl^-$ (data not shown) as well as in excised outside-out patch clamp recordings with external $SCN^-$ to increase the current amplitudes (data not shown) we observed a pronounced rectification of the instantaneous current amplitude. However, it is still possible that gating
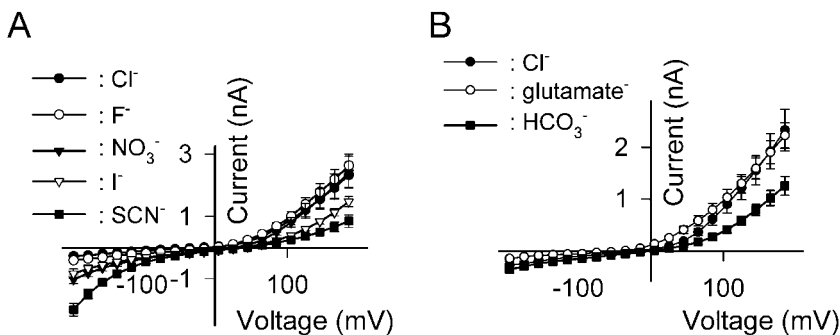
A



B



FIGURE 5 Instantaneous current amplitudes for various internal solutions. (*A*) Voltage-dependence of instantaneous current amplitudes determined after a 200 ms prepulse to +75 mV for different anion compositions. Current amplitudes were measured in cells perfused with a solution containing (in mM): 120 NaX, 5 EGTA, 10 HEPES, pH 7.4; $X^-$ denotes $I^-$, $SCN^-$, $NO_3^-$, or $F^-$. The external solution had the standard composition. (*B*) Voltage-dependence of instantaneous current amplitudes determined after a 200 ms prepulse to +75 mV for additional internal anions, such as glutamate and $HCO_3^-$. Mean $\pm$ SE from 5 to 10 cells.

steps faster than the clamp speed of these methods exist and are responsible for the observed rectification.

To test for such a possibility we used variance analysis. We determined the isochronal current amplitude and the isochronal current variance at test potentials between $-100$ mV and $+175$ mV immediately after the setting of the capacitive gradient (1 ms after the voltage; see Fig. 2 $A$). For each test potential, a series of identical records was recorded and pairs of subsequent records were subtracted to compute the ensemble variance. Later, the noise ($\sigma_o^2$) measured at the reversal potential was subtracted, and variances determined at various potentials were plotted versus the mean current amplitude determined at the same time (Fig. 2 $B$). This plot could be well fit with a parabolar function (*solid line*). Fig. 2 $C$ shows averaged data from a total of seven experiments. Isochronal current amplitudes and variances were normalized to the respective values at $+125$ mV. The solid line represents a fit of $y = ax^2$ to these averaged data that represents well the experimental data. The quality of the fit was evaluated by plotting the square root of the normalized noise versus the normalized current amplitudes (Fig. 2 $C$, *insert*). This plot could be well fit with a straight line passing through the origin ($r^2 = 0.96$).

In such a plot (see Materials and Methods), the isochronal standard deviation of current fluctuations for $N$ channels depends on the corresponding mean current $I$ according to Eq. 4:

$$\sigma(V) = I(V)\sqrt{\frac{(1/p(V)) - 1}{N}}.$$

Fig. 2 demonstrates that for all voltages between $-100$ mV and $+175$ mV, the isochronal standard deviation and the isochronal current amplitude are proportional to each other. Thus, for all tested voltages, the isochronal open probability is constant indicating that the unitary current amplitude is proportional to the isochronal current amplitude. Our test established that human ClC-4 channels display a voltage-dependent single channel conductance that fully accounts for the observed macroscopic rectification.

If macroscopic rectification arose from gating processes, the open probability would be different for various voltages, i.e., it must increase with more depolarized test pulses. Our analysis is capable to distinguish an open channel rectification from a gating rectification (Fig. 2 $D$). Isochronal current-noise relationships (*dashed lines*) were calculated assuming that the unitary conductance is constant and that the macroscopic rectification is caused by changes of the absolute open probability. The simulations were done for an isochronal absolute open probability of 0.7 (*thin line*) and of 0.1 (*thick line*) at $+175$ mV, using the experimentally observed current amplitudes shown in Fig. 2 $A$ and the experimentally determined variance at $+175$ mV. For both cases, simulated variance-mean current plots substantially differed from the experimental results ($\bullet$).

## Unitary current amplitude of ClC-4 channels

We next determined single channel amplitudes by nonstationary noise analysis. In standard internal and external solutions, the activating current component was only very small, i.e., the channels' open probability changed only little with time and this virtually prevented reliable fits with Eq. 7 under these conditions. However, with a standard external solution and an internal solution in which $Cl^-$ was completely substituted with $I^-$, nonstationary noise analysis was possible (Fig. 3, $A$–$D$).

Fig. 3, $A$–$C$ shows variance analysis from a tsA201 cell expressing ClC-4 channels perfused with internal iodide solution in standard external solution. Fig. 3, $A$ and $B$ illustrate the time course of the average current for a voltage step from a holding potential of 0 mV to a test potential of $+140$ mV and the corresponding time course of the variance. To obtain the unitary current amplitude of the underlying channels at this potential, the variance-mean current plot in Fig. 3 $C$ was fitted to Eq. 7 (see Materials and Methods). From this fit, the unitary current amplitude, $i = 0.085$ pA at $+140$ mV, and the number of channels in the cell (28,672), were obtained. We then calculated the open probability at the beginning of the test pulse (0.27), by dividing the instantaneous current amplitude by the product of the unitary current amplitude and the number of channels, and the open probability at the end of the test pulse (0.71), by dividing the late current amplitude by the same product. Measurements were repeated in several cells at four different test potentials. Within this limited voltage range, the rectification of the single channel amplitude was very similar to the instantaneous macroscopic current amplitude rectification under identical ionic conditions (Fig. 3 $D$) in agreement with the conclusion of the previous paragraph.

Because the open probability of ClC-4 is distinct from zero at the beginning of the test pulse, the variance-mean current plot is not a complete parabola. However, as the fitted parabola assumed its maximum within the experimentally determined variance-mean current plot, the fits were well defined. We obtained reproducible results for the unitary
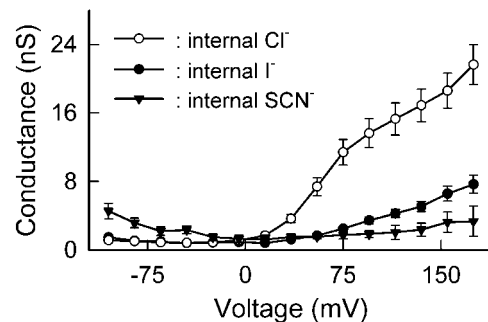


FIGURE 6 Instantaneous conductance at various internal solutions. Voltage-dependence of the mean absolute conductance mean $\pm$ SE from at least seven cells perfused with an internal solution containing $Cl^-$ ($\bigcirc$), $I^-$ ($\bullet$), and $SCN^-$ ($\blacktriangledown$) as the main anion.

current amplitude and the open probabilities at the beginning and the end of the voltage step in several cells. Moreover, the voltage-dependence of the calculated single channel amplitudes is in close correlation with instantaneous macroscopic current amplitude (Fig. 3 *D*). All these results demonstrated that our nonstationary noise analysis reliably determined the unitary channel amplitude of ClC-4.

## Anion selectivity of ClC-4

ClC channels are permeable to various anions, and permeant anions provide a simple tool to get insights into the function of the ion conduction pathway. We therefore measured ClC-4 currents using whole-cell recordings on tsA201 cells under several asymmetric anionic conditions.

We first studied the instantaneous current-voltage relationships in the presence of various external anions. Currents were recorded in a solution containing 150 mM NaCl and 5 HEPES, and later brought into the stream of a perfusion system with various solutions in which NaCl was completely substituted with several sodium salts. Fig. 4 *A* shows the voltage-dependence of the normalized instantaneous current amplitude determined after an activating prepulse to +75 mV for $Br^-$, $I^-$, $F^-$, $NO_3^-$, $N_3^-$, and $SCN^-$, and Fig. 4 *B* for $HCO_3^-$, $CH_3COO^-$, $CH_3SO_3^-$ (methane sulfonate$^-$), and glutamate$^-$. Except glutamate, all tested anions permeated

well. Current amplitudes at positive potentials were largest for polyatomic anions such as $N_3^-$, $NO_3^-$, and $SCN^-$; they differed only slightly among halides such as $Cl^-$, $Br^-$, $I^-$, and $F^-$. In contrast to ClC-1 (Rychkov et al., 1998), $HCO_3^-$ and $CH_3SO_3^-$ were measurably permeant through ClC-4 channels.

ClC-4 did not express in sufficient density to use macroscopic recordings from excised inside-out patches for studying the effects of several internal anions at the same population of channels. However, different cells exhibited quite similar whole cell current amplitudes (Fig. 5) that allowed comparisons of current amplitudes between different populations of cells. Fig. 5 *A* presents averaged instantaneous current amplitudes for cells intracellularly perfused with solutions containing $Cl^-$, $I^-$, $F^-$, $NO_3^-$, and $SCN^-$, and Fig. 5 *B* with glutamate$^-$ and $HCO_3^-$ as the only internal anion.

Compared with $Cl^-$, all other permeant anions exhibited a larger relative inward current at negative potentials. With $I^-$, $NO_3^-$, and $SCN^-$ as internal anions, the current-voltage relationship is clearly bidirectionally rectifying. The chloride influx at positive potentials was little affected by exchanging the internal anion composition to $F^-$, $NO_3^-$, glutamate$^-$, and $HCO_3^-$, but internal $SCN^-$ and $I^-$ significantly reduce $Cl^-$ influx. This is further illustrated in Fig. 6, where averaged anion conductances from cells perfused with internal $Cl^-$, $I^-$, and $SCN^-$ are shown. The absolute values as well as the voltage-dependence of the macroscopic conductance at positive potentials were distinct for cells perfused with $Cl^-$, $I^-$, or $SCN^-$ indicating block of chloride currents by $I^-$ and $SCN^-$.

## Conductivity and permeability sequences in ClC-4

From the results described above we determined conductivity sequences for external ($SCN^- > N_3^- > NO_3^- > Cl^- \sim F^- \sim I^- > Br^- > HCO_3^- > CH_3SO_3^- > CH_3COO^- > Glutamate^-$) and for internal anions ($SCN^- > NO_3^- > I^- > F^- > HCO_3^- > Cl^- \gg Glutamate$); see Fig. 7 *A*.

So far, current reversal potentials and permeability ratios have not been determined for ClC-4. There was uncertainty whether these channels are active at negative potentials. As the macroscopic conductance by ClC-4 channels is small at these potentials, a major contribution of non-ClC-4 current components to the setting of the whole-cell reversal potential could not be excluded.

Variance analysis now demonstrated that ClC-4 channels are active over the whole voltage range. Moreover, a substantial contribution of endogenous or leakage conductances could be ruled out because of the following observations. The macroscopic conductances measured in cells expressing hClC-4 at the reversal potential were larger than in untransfected cells for all ionic conditions. Reversal potentials in transfected cells were distinct from those determined in untransfected cells. If endogenous currents were a major
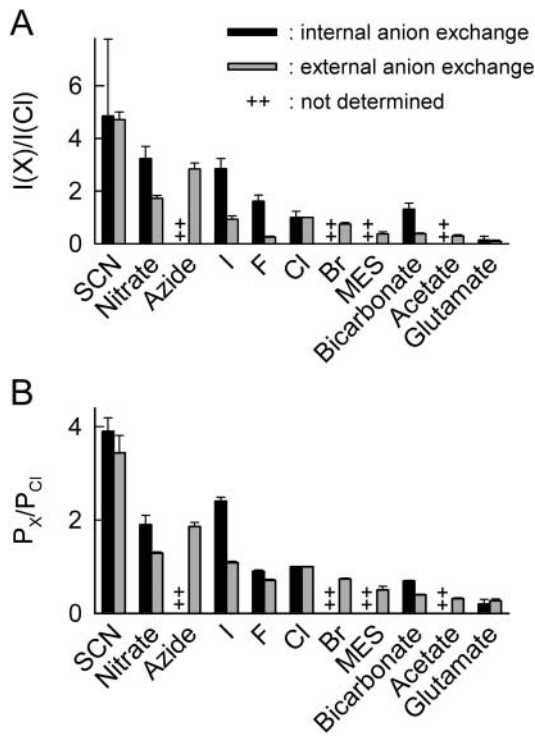


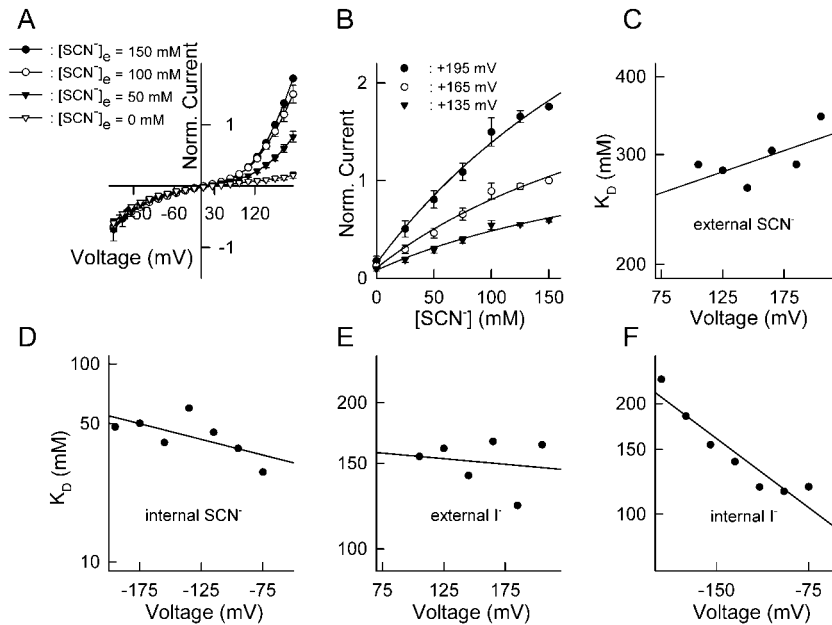FIGURE 7 Anionic selectivity of ClC-4. (*A*) Relative current amplitude at +125 mV. (*B*) Relative permeability.

FIGURE 8  Effect of changes of the external and internal $SCN^-$ or $I^-$ concentration on instantaneous current amplitudes in tsA201 cells expressing ClC-4. For changes of external $[SCN^-]$, cells were perfused with a solution containing (in mM): 123 NaSCN, 5 EGTA, 10 HEPES, pH 7.4. For comparison of various internal solutions, the external solution was always containing (in mM) 150 NaSCN, 5 HEPES, pH 7.4. (*A*) Mean current amplitudes for various external $[SCN^-]$. $SCN^-$ was substituted equimolarly with glutamate. For exchange of the external solution, data were normalized to the current amplitude measured at +165 mV at $[SCN^-]_e = 150$ mM; for internal concentrations, absolute current amplitudes were averaged. (*B*) Concentration dependence of instantaneous current amplitudes for changes of external $[SCN^-]$. Solid lines represent fits to the Hill equation. (*C*) Voltage-dependence of the $K_D$ obtained from the Hill fits shown in *B* in a semilogarithmic plot. (*D–F*) Voltage-dependence of the $K_D$ obtained from Hill fits similar to those shown in *B* for variation of internal $[SCN^-]$ (*D*), external $[I^-]$ (*E*) or internal $[I^-]$ (*F*) in a semilogarithmic plot.

determinant of the reversal potential, one would expect a correlation between the channel density, i.e., the maximum current amplitude, and the measured reversal potential. Such a correlation was not observed (data not shown) indicating that the experimentally determined reversal potentials reliably report the selectivity of ClC-4 channels.

Reversal potentials from the experiments described in the previous paragraph could therefore be used to calculate permeability coefficients of hClC-4 (Fig. 7 *B*). The permeability for external anions decreased in the order of $P_{SCN} > P_{NO3} > P_{N3} > P_I \sim P_F \sim P_{Cl} > P_{Br} > P_{CH3SO3} > P_{HCO3} > P_{CH3COO} > P_{glutamate}$ (Table 1), and for internal, in the order of $P_{SCN} > P_I > P_{NO3} > P_{Cl} = P_F > P_{HCO3} > P_{glutamate}$ (Table 2). The relative permeability values for internal anions were distinct from those calculated from experiments in which the external concentration was exchanged, indicating multiple occupancy of the ClC-4 pore (Fig. 8 *A*; see also McGill and Schumaker, 1995).

## Concentration dependence for external and internal $SCN^-$ and $I^-$

We next studied ClC-4 whole-cell currents under various internal and external $SCN^-$ concentrations. Fig. 8 *A* shows averaged normalized instantaneous current amplitudes at various voltages after an activating prepulse to +75 mM for four distinct external $[SCN^-]$. When altering the external $[SCN^-]$, $SCN^-$ was equimolarly substituted with glutamate. Whereas alteration of external $[SCN^-]$ had little effect on the current amplitudes at negative potentials, the current amplitudes in the positive voltage range increased with $[SCN^-]$. In Fig. 8 *B*, the concentration-current amplitude relationship is given for three test pulse potentials, +135 mV,

+165 mV, and +195 mV. In all cases, a Michaelis-Menten relationship with a Hill coefficient of 1 could adequately describe the data, providing dissociation constants ($K_D$) in the range between 250 and 330 mM (Fig. 8 *C*).

Our analysis was performed at voltages more than 80 mV away from the current reversal potential. For a multiply-occupied channel ($n > 1$), the ratio of efflux divided by influx is negligible under these conditions ($j_{eff}/j_{in} = e^{-n(E-E_{ref})/RT}$ where $n$ is the number of simultaneously binding ions (Hodgkin and Keynes, 2002)). The concentration dependence of the current thus described the concentration dependence of the ion influx. Saturation of the ion influx with increasing external $[SCN^-]$ occurs when the binding-unbinding step to the first binding site within the ion conduction pathway becomes rate-limiting. This happens when the rate of entry approaches the maximum rate of the unbinding step. Unbinding can occur by passing through the pore ($k_{trans}$) or by diffusing into the external solution ($k_{off}$). The dissociation constants (Fig. 8 *C*) thus depend on $k_{trans}$ and $k_{off}$ as well as on the rate constant for entering the binding site ($k_{on}$) from the external solution ($K_D = (k_{off} + k_{trans})/k_{on}$).

The determined dissociation constants were only slightly voltage dependent, and increased with more positive potentials. At more depolarized potentials, $k_{on}$ and $k_{trans}$ are expected to increase, whereas $k_{off}$ exhibits the inverse voltage-dependence. The experimentally observed voltage-dependence of $K_D$ thus implies that the rate constant for translocating through the pore ($k_{trans}$) is large compared with $k_{on}$ and $k_{off}$. Translocation through the ion conduction pathway is fast compared with entering/leaving the ion conduction pathway. Obviously, the association to the external binding site is the rate-limiting step during the inward movement of $SCN^-$.

For a similar analysis with variation of internal [SCN$^-$], we compared measurements from multiple cells under various internal solutions. There is a clear increase of anion outward current at negative potentials with higher [SCN$^-$]$_{int}$, and current amplitudes at positive potentials are largest for the smallest concentration of internal SCN$^-$. We again plotted current amplitudes at fixed potentials versus [SCN$^-$], and fitted this plot with a Hill relationship. The calculated $K_D$s are given in Fig. 8 *D*, they were smaller than the $K_D$ determined for variation of the external [SCN$^-$]. There was again the paradox voltage-dependence of the dissociation constants that increase with more negative potentials. This experiment was repeated for external and internal iodide (Fig. 8, *E* and *F*) providing qualitatively similar results.

## DISCUSSION

### ClC-4 channels exhibit a very small single channel amplitude

We used nonstationary noise analysis to determine the unitary conductance of ClC-4. Variance analysis of ClC-4 currents was only possible in ionic conditions distinct from our standard recording solutions, and under these conditions, single channel current amplitudes were very low, i.e., below 0.1 pA at potentials positive to +100 mV. Variance analysis is complicated by the unique architecture of this channel. ClC channels exhibit two identical ion conduction pathways per channel (Miller, 1982; Dutzler et al., 2002), most likely resulting in the occurrence of two equally spaced subconductance state in all ClC isoforms. The existence of more than one conductance states violates the assumptions for Eq. 7 and may thus lead to incorrect estimates of the single channel amplitudes. To get an approximation of the possible error introduced by this uncertainty, we performed simulations with modeled channels that exhibited two equally spaced subconductance states. Using our standard noise analysis, we determined a unitary current amplitude that is between the simulated half- and the full-conductance state.

As activation gating was only observed at very positive potentials, we could not determine unitary current amplitudes for less positive or even negative potentials using nonstationary noise analysis. Instead, we used a modification of the variance analysis to get information about unitary current amplitudes at hyperpolarized membrane voltages (Fig. 2). A plot of the variance versus the instantaneous current amplitude demonstrated that ClC-4 displays an open channel rectification similar to the rectification of the instantaneous macroscopic current amplitude (Fig. 1 *B*).

In a recent publication, Vanoye and George (2002) reported single channel recordings from mammalian cells heterologously expressing ClC-4 with unitary conductances that were substantially larger than our estimates based on noise analysis. At +60 mV, these channels had a single

channel amplitude of ~0.15 pA in symmetrical Cl$^-$. The open probability was very low at +40 mV and +60 mV. Moreover, channel openings were not visible at negative membrane potentials. Such a channel would not produce variance-current amplitude relationships as shown in Figs. 2 and 3. Therefore, the single channel conductance as well as the voltage-dependence of the open probability of these channels differ from our nonstationary noise analysis.

A possible source of error for determining the unitary current amplitude by noise analysis is a potential contribution of endogenous current amplitudes to the observed noise. For the following reasons, we are convinced that such an error does not affect the determination of the ClC-4 unitary conductance in our experiments. Firstly, we determined noise in nontransfected cells obtaining values that were significantly lower than those observed in transfected cells. Secondly, the analysis shown in Fig. 2 demonstrates a linear relationship between the square root of the variance and the hClC-4 specific current amplitude over the whole voltage range. This virtually excludes a contribution of Lorentzian noise generated by the observed linear background conductance. Because of the pronounced rectification of hClC-4 currents, a contribution of background noise would be more pronounced in the negative than in the positive voltage range. This would cause a deviation from the linear relationship between the standard deviation and the mean current amplitude resulting in two straight lines with distinct slopes at negative and at positive voltages. Because of the distinct relative endogenous current amplitudes, the relative deviation ratio of these slopes would vary from cell to cell. Lastly, a contribution of background noise would increase the absolute value of the variance and therefore cause an overestimation of the unitary current amplitude by variance analysis.

All these lines of evidence support the notion that hClC-4 channels indeed exhibit a very small single channel amplitude under our experimental conditions. At present, we cannot explain the different outcomes of the two studies. As the expression system (tsA201 cells) as well as the coding region of the expressed construct (obtained as the I.M.A.G.E. ID 712030 EST clone) are identical, differences in the coding region or the molecular assembly of the channels in this and in the earlier study appear very unlikely. Two distinct recordings modes were used, excised patches (Vanoye and George, 2002) or whole-cell recordings, respectively. Inasmuch as functional alterations induced by the patch formation or patch excision were reported for certain channels (Fahlke and Rüdel, 1992; Sigg et al., 2002), this might account for the observed differences. In both experimental approaches, ATP was omitted from the internal solution allowing rundown of the ClC-4 current. Assuming that ClC-4 rundown does not simply reduce the number of functional channels, but modifies its functional properties, it appears possible that the observed single channels are in a distinct functional state than the channels in the whole-cell current recordings. A

rundown process that affects the conduction as well as the gating properties of ClC-4 channels might explain the observed differences in single channel amplitude. Alternatively, the single channel recordings might represent anion channels endogenous to the expression system that are upregulated by the heterologous expression of ClC-4.

## Physiological implications of the functional features of ClC-4

Nonstationary noise analysis demonstrated that ClC-4 exhibited an open probability distinct from zero over the whole voltage range. The prominent outward rectification is due to a pronounced voltage-dependence of the unitary current amplitude, whereas the activation gating at positive potentials causes a limited increase of the absolute open probability. Our findings have important physiological implications. Previously, many authors have assumed that rectification of ClC-4, and also of the closely related ClC-5, is due to a particular gating of these channels causing complete closure at negative potentials. Channels with such a gating behavior would not be able to conduct anion currents large enough to exert a physiological effect (Jentsch and Günther, 1997; George et al., 2001; Mohammad-Panah et al., 2001). Our findings now establish that ClC-4 is active at negative potentials and can conduct anions through the external cell membrane as well as through the membrane of internal cell compartments. Thus, this ClC isoform is able to fulfill various physiological tasks even without modulating cofactors that might alter its gating.

## ClC-4 exhibits at least two distinct binding sites that can be simultaneously occupied

ClC-4 exhibits a multiply-occupied ion conduction pathway. $SCN^-$ and $I^-$ blocked anion currents when applied from the inside, but $SCN^-$ enhanced the current when applied from the outside (Figs. 4, 5, 8), indicating that there are at least two qualitatively distinct binding sites. For $I^-$, $NO_3^-$, and $HCO_3^-$, the relative anion permeability ratio depends on the side of the membrane to which the anion was applied (Fig. 7). Although such a feature is observed in multiply-occupied channels, it is also feasible in singly occupied channels with voltage-dependent permeability ratios (Hille, 1992). However, the result that for other anions such as $SCN^-$, the permeability ratio was basically the same for internal and external application, eliminated this possibility.

The binding sites within the ClC-4 pore all prefer large and polyatomic anions (lyotropic binding sites), but they differ in the apparent absolute interaction energy with anions. $SCN^-$ ions bind to the internal side tightly enough to block anion flux through ClC-4 (Fig. 5), whereas application of the same anion to the external side of the membrane increases the current (Fig. 4).

The existence of more than one lyotropic binding site seems to be a general feature of ClC channels. The muscle isoform ClC-1 also exhibits at least two distinct anion binding sites that can be simultaneously occupied by more than one anion (Fahlke et al., 1997a,b; Rychkov et al., 1998). However, larger and polyatomic anions block this isoform from both sides of the membrane with lower $K_D$s than was observed for ClC-4 (Fahlke et al., 1997a). Obviously, binding sites within the ClC-1 and the ClC-4 ion conduction pathways differ in absolute interaction energy with anions.

## Anion selectivity of ClC channels

ClC-4 exhibits pore properties that are distinct from ClC-0, -1, and -2 (Fahlke, 2001). For ClC-0, -1, and -2, $Cl^-$ is the anion with the highest conductance and permeability. Larger and polyatomic anions block $Cl^-$ currents through these isoforms from either side of the membrane and display smaller relative conductance and permeabilities. Despite these differences, fundamental pore properties, like multiple occupancy and the binding selectivity of the anion binding sites, seem to be conserved.

In the following, we will try to develop a model that takes the specific functional features of various ClC isoforms and recent crystallographic results into account. The atomic structure of two prokaryotic ClC channels, from *S. typhimurium* and from *E. coli* (Dutzler et al., 2002), provided insight into the mechanisms by which probably all ClC channels select between anions and cations and into the permeation process of anions. The crystal structure showed one anion in each ion conduction pathway that is cooperatively bound by several highly conserved protein regions and electrostatically stabilized by the dipole moment of the helices D, F, and N (Dutzler et al., 2002). As there is only one bound anion in the ClC channel structure, the multiple occupancy of ClC-1 and ClC-4 is most likely due to the existence of additional low-affinity binding sites that are not visible in the crystal structure. A simple model that explains the structural and functional data is an ionic pore with one high-affinity binding site (the one visible in the StClC structure) and two adjacent low-affinity binding sites that are responsible for multiple occupancy and for isoform-specific differences in anion selectivity. Dang and McCleskey (1999) demonstrated that a stepwise permeation model with one high-affinity binding site flanked on both sites with low-affinity sites predicts the same ion conduction properties as a doubly occupied pore with interaction between the two binding sites (Hess and Tsien, 1984; Almers and McCleskey, 1984; Kiss et al., 1998). Such a model thus accounts for the functional indications of multiple occupancy in ClC-1 and ClC-4.

In the framework of such a model, the peripheral anion binding sites appear to be crucial in determining the particular pore properties of ClC channels. The functional
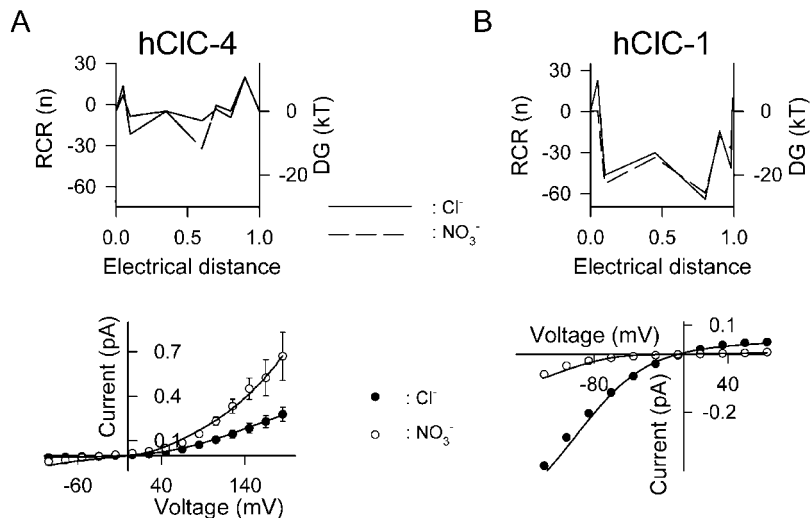
FIGURE 9 Results of fits with a four-barrier model to the voltage-dependence of unitary current amplitudes for ClC-4 (*A*) and ClC-1 (*B*). Fits were performed for two external solutions—the standard solution (●) and a solution in which NaCl was completely substituted with NaNO$_3$ (○). Fit parameters are shown as reduced rate constant representation (*RCR*) and as $\Delta G$, following Andersen (1999).

characteristics of ClC-1 (Fahlke et al., 1997a,b; Rychkov et al., 1998) and ClC-4 reveal that these sites prefer large and polyatomic anions, i.e., they are lyotropic anion binding sites. Differences in the absolute interaction energy with anions of these binding sites appear to be responsible for isoform-specific pore properties of ClC-1 and ClC-4. In ClC-1, the rate-limiting step in anion permeation is the dissociation of anions from one of these sites (Fahlke, 2001). Anions that bind with higher affinity dwell longer at these sites, and this reduces their mobility within the pore. For this reason, ClC-1 exhibits a permeability sequence that is the inverse of a lyotropic selectivity sequence (Fahlke et al., 1997a,b). In contrast, in ClC-4, the association of permeant anions to one of these binding sites is the rate-limiting step in ion permeation (Fig. 8). The permeability sequence follows the affinity sequence of the binding sites, and larger and polyatomic anions exhibit a higher permeability than other anions. Block of anion flux by other permeant anions is therefore not very pronounced in ClC-4.

To test whether such a three-binding-site model can account for the voltage-dependence and selectivity of the unitary current amplitudes, we fitted a sequential state model without electrostatic interaction to experimentally determined unitary current amplitudes of ClC-4 and ClC-1. These fits were performed for two ionic conditions, standard external and internal solutions, as well as standard internal solution and an external solution in which the NaCl was completely substituted with equimolar NaNO$_3$. They provide reasonably good approximations of the experimentally observed results, i.e., the particular rectification of ClC-4 and ClC-1, the block of ClC-1 currents as well as the enhancement of ClC-4 currents in NO$_3^-$. The values of the rate constants can be represented graphically by depicting energy barriers and wells inferred from these rates (Andersen, 1999; see also Fig. 9). The absolute values of the free energies depend on the value of a frequency factor

used for the calculation of individual rate constants (Andersen, 1999) that cannot be determined experimentally. However, the values we are most interested in, the differences of the barrier heights and the distinct wells, are invariant for various frequency factors. We therefore chose for simplicity a prefactor of $6 \times 10^{12}$ s$^{-1}$ ($= kT/h$). The so-obtained graphic presentation of rate constants and the deduced barrier and well heights nicely illustrates the plausibility of our qualitative reasoning about the functional differences between ClC-4 and ClC-1. Clearly, a sequential model with rate-limiting dissociation rate constants in permeation through ClC-1 and rate-limiting association rate constants for ClC-4 predicts rectification, selectivity and block in these two isoforms (Fig. 9).

Based on this barrier model as well as on the qualitative arguments listed above, the distinct anion selectivity of ClC-1 and ClC-4 can be intuitively explained by assuming differences in the electrostatic potential within the ion conduction pathway. ClC-4 exhibits a less positive electrostatic potential than ClC-1, decreasing the association rate constant to the anionic binding sites and making it rate-limiting. This scenario explains the differences in relative anion permeability, the smaller unitary conductance of ClC-4, the less pronounced block by permeant anions, and the paradoxical voltage-dependence and the larger values of K$_{DS}$ of I$^-$ and SCN$^-$ currents. We can currently only speculate about the possible molecular basis of these isoform-specific properties. Using site-directed mutagenesis, it has been recently established that fixed charges play a role in determining the absolute binding affinity for ClC-1. Neutralizing K231 (located in the N-terminus of the F-helix) by substituting a cysteine causes an inversion of the Cl > *I* permeability of WT ClC-1. Restoring the positive charge by reacting a MTSEA reagent to C231 restores the selectivity and the block by larger and polyatomic anions (Fahlke et al., 1997c). It thus appears conceivable that an altered relative

position of this charged side chain in ClC-4 is one reason for differences in anion selectivity. Alternatively, additional fixed charges close to the ClC-1 selectivity filter or an altered spatial arrangement of the helices *D*, *F*, and *N* forming the ClC selectivity filter in ClC-1 and ClC-4 might also result in the observed differences in the electrostatic potential.

In addition, ClC-4 seems to have a larger pore diameter than ClC-1. In contrast to ClC-1, ClC-4 conducts $CH_3SO_3^-$ as well as $F^-$. In ClC-1, $F^-$ is thought to be impermeant because the weak interacting binding sites within the ion conduction pathway do not provide sufficient interaction energy to dehydrate this anion. The hydrated $F^-$ is too large to pass the pore narrowing of this isoform (Fahlke, 2001). $CH_3SO_3^-$ is thought to be impermeant through ClC-1 because the size of the dehydrated anion is larger than the channel constriction. It binds with higher affinity than $Cl^-$ to the external binding site (Fahlke et al., 1997b), but cannot move through the pore narrowing. The differing functional features of ClC-4 are most likely due to a considerably larger pore narrowing than in ClC-1.

The apparent differences in the size of the pore narrowing as well as in the electrostatic potential between ClC-1 and ClC-4 suggests that functional properties of the selectivity filter are not completely conserved within the ClC family. Based on this finding one might speculate about a certain variation of structural features of this channel region in distinct ClC channels.

## CONCLUSIONS

ClC-4 exhibited unique ion permeation properties: a very small unitary current amplitude, a pronounced unitary current rectification, and an anion selectivity that is distinct from other ClC channels. Despite these differences, the ion conduction pathway of ClC-4 exhibits typical ClC channel features, i.e., it has a multiply-occupied pore with at least two lyotropic anion binding sites. Our results are in agreement with the notion that anion conductivity and permeability in ClC-type chloride channels are governed by association to and dissociation from several anionic binding sites that exhibit lyotropic selectivity sequences, but differ in their absolute binding affinity between distinct anion channels.

## REFERENCES

Almers, W., and E. W. McCleskey. 1984. Nonselective conductance in calcium channels of frog muscle: calcium selectivity in a single-file pore. *J. Physiol. (Lond.)*. 353:585–608.

Alvarez, O., C. Gonzalez, and R. Latorre. 2002. Counting channels: a tutorial guide on ion channel fluctuation analysis. *Adv. Physiol. Educ.* 26:327–341.

Andersen, O. S. 1999. Graphic representation of the results of kinetic analyses. *J. Gen. Physiol.* 114:589–590.

Barry, P. H. 1994. JPCalc, a software package for calculating liquid junction potential corrections in patch-clamp, intracellular, epithelial and bilayer measurements and for correcting junction potential measurements. *J. Neurosci. Methods.* 51:107–116.

Dang, T. X., and E. W. McCleskey. 1999. Ion channel selectivity through stepwise changes in binding affinity. *J. Gen. Physiol.* 111:185–193.

Dutzler, R., E. D. Campbell, M. Cadene, M. B. Chait, and R. MacKinnon. 2002. X-ray structure of a ClC chloride channel at 3.0 A reveals the molecular basis of anion selectivity. *Nature.* 415:287–294.

Fahlke, Ch. 2001. Ion permeation and selectivity in ClC-type chloride channels. *Am. J. Physiol. Renal Fluid Electrol. Physiol.* 280:F748–F757.

Fahlke, Ch., C. L. Beck, and A. L. George, Jr. 1997a. A mutation in autosomal dominant myotonia congenita affects pore properties of the muscle chloride channel. *Proc. Natl. Acad. Sci. USA.* 94:2729–2734.

Fahlke, Ch., C. Dürr, and A. L. George, Jr. 1997b. Mechanism of ion permeation in skeletal muscle chloride channels. *J. Gen. Physiol.* 110:551–564.

Fahlke, Ch., and R. Rüdel. 1992. Giga-seal formation alters properties of sodium channels of human myoballs. *Pflugers Arch.* 420:248–254.

Fahlke, Ch., H. T. Yu, C. L. Beck, T. H. Rhodes, and A. L. George, Jr. 1997c. Pore-forming segments in voltage-gated chloride channels. *Nature.* 390:529–532.

Friedrich, T., T. Breiderhoff, and T. J. Jentsch. 1999. Mutational analysis demonstrates that ClC-4 and ClC-5 directly mediate plasma membrane currents. *J. Biol. Chem.* 274:896–902.

George, A. L., M. A. Crackower, J. A. Abdalla, A. J. Hudson, and G. C. Ebers. 1993. Molecular basis of Thomsen's disease (autosomal dominant myotonia congenita). *Nat. Genet.* 3:305–310.

George, A. L., Jr., L. Bianchi, E. M. Link, and C. G. Vanoye. 2001. From stones to bones: the biology of ClC chloride channels. *Curr. Biol.* 11:R620–R628.

Hamill, O. P., A. Marty, E. Neher, B. Sakmann, and F. J. Sigworth. 1981. Improved patch-clamp techniques for high-resolution current recording from cells and cell-free membrane patches. *Pflugers Arch.* 391:85–100.

Heinemann, S. H., and F. Conti. 1992. Nonstationary noise analysis and application to patch clamp recordings. *Method Enzymol.* 207:131–148.

Hess, P., and R. W. Tsien. 1984. Mechanism of ion permeation through calcium channels. *Nature.* 309:453–456.

Hille, B. 1992. Ionic Channels of Excitable Membranes. Sinauer Associates Inc., Sunderland, MA.

Hodgkin, A. L., and R. D. Keynes. 2002. The potassium permeability of a giant nerve fibre. *J. Physiol. (Lond.)*. 128:61–88.

Jentsch, T. J., and W. Günther. 1997. Chloride channels: an emerging molecular picture. *Bioessays.* 19:117–126.

Jentsch, T. J., W. Günther, M. Pusch, and B. Schwappach. 1995. Properties of voltage-gated chloride channels of the ClC gene family. *J. Physiol. (Lond.)*. 482:19S–25S.

Jurman, M. E., L. M. Boland, Y. Liu, and G. Yellen. 1994. Visual identification of individual transfected cells for electrophysiology using antibody-coated beads. *Biotechniques.* 17:876–881.

Kawasaki, M., T. Fukuwa, K. Yamauchi, H. Sakamoto, F. Marumo, and S. Sasaki. 1999. Identification of an acid-activated $Cl^-$ channel from human skeletal muscle. *Am. J. Physiol. Renal Physiol.* 46:C948–C954.

Kiss, L., D. Immke, J. LoTurco, and S. J. Korn. 1998. The interaction of Na$^+$ and K$^+$ in voltage-gated potassium channels. Evidence for cation binding sites of different affinity. *J. Gen. Physiol.* 111:195–206.

Koch, M. C., K. Steinmeyer, C. Lorenz, K. Ricker, F. Wolf, M. Otto, B. Zoll, F. Lehmann-Horn, K. H. Grzeschik, and T. J. Jentsch. 1992. The skeletal muscle chloride channel in dominant and recessive human myotonia. *Science.* 257:797–800.

Kornak, G., D. Kasper, M. R. Boesl, E. Kaiser, M. Schweizer, A. Schulz, W. Friedrich, G. Delling, and T. J. Jentsch. 2001. Loss of the ClC-7 chloride channel leads to osteopetrosis in mice and man. *Cell.* 104:205–215.

Lloyd, S. E., S. H. S. Pearce, S. E. Fisher, K. Steinmeyer, B. Schwappach, S. J. Scheinman, B. Harding, B. Alessandra, P. Devota, P. Goodyear, S. P. A. Rigden, O. Wrong, T. J. Jentsch, I. W. Craig, and R. V. Thakker. 1996. A common molecular basis for three inherited kidney stone diseases. *Nature.* 379:445–449.

McGill, P., and M. F. Schumaker. 1995. Orientation independence of single-vacancy and single-ion permeability ratios. *Biophys. J.* 69:84–93.

Miller, C. 1982. Open-state substructure of single chloride channels from *Torpedo* electroplax. *Philos. Trans. R. Soc. Lond. B Biol. Sci.* 299:401–411.

Mindell, J. A., D. J. Pheasant, and C. Miller. Currents for human ClC-4 expressed in *Xenopus* oocytes and cultured mammalian cells. *Biophysical Journal* 74[2], A222. 1998.

Mohammad-Panah, R., C. Ackerley, J. M. Rommens, M. Choudhury, and C. E. Bear. 2001. The chloride channel ClC-4 co-localizes with CFTR and may mediate chloride flux across the apical membrane of intestinal epithelia. *J. Biol. Chem.* 277:566–574.

Neher, E. 1992. Correction for liquid junction potentials in patch clamp experiments. *Method Enzymol.* 207:123–131.

Rosenbohm, A., R. Rüdel, and Ch. Fahlke. 1999. Regulation of the human skeletal muscle chloride channel hClC-1 by protein kinase C. *J. Physiol. (Lond.).* 514:677–685.

Rychkov, G. Y., M. Pusch, M. L. Roberts, T. J. Jentsch, and A. H. Bretag. 1998. Permeation and block of the skeletal muscle chloride channel, ClC-1, by foreign anions. *J. Gen. Physiol.* 111:653–665.

Sigg, D., F. Bezanilla, and E. Stefani. 2002. Slowing of deactivation kinetics in *Shaker* B as seen in macropatch recordings of gating and ionic currents. *Biophys. J.* 66:A439.

Simon, D. B., R. S. Bindra, T. A. Mansfield, C. Nilson-Williams, E. Mendonca, R. Stone, S. Schurman, A. Nayir, H. Alpay, A. Bakkaloglu, J. Rodriguez-Soriano, J. M. Morales, S. A. Sanjad, C. M. Taylor, D. Pilz, A. Brem, H. Trachtman, W. Griswold, G. A. Richard, E. John, and R. P. Lifton. 1997. Mutations in the chloride channel gene, *CLCNKB*, cause Bartter's syndrome type III. *Nat. Genet.* 17:171–178.

Stobrawa, S. M., T. Breiderhoff, S. Takamori, D. Engel, M. Schweizer, A. A. Zdebik, M. R. Bosl, K. Ruether, H. Jahn, A. Draguhn, R. Jahn, and T. J. Jentsch. 2001. Disruption of ClC-3, a chloride channel expressed on synaptic vesicles, leads to a loss of the hippocampus. *Neuron.* 29:185–196.

van Slegtenhorst, M. A., M. T. Bassi, G. Borsani, M. C. Wapenaar, G. B. Ferrero, L. de Conciliis, E. I. Rugarli, A. Grillo, B. Franco, and H. Y. Zoghbi. 1994. A gene from the Xp22.3 region shares homology with voltage-gated chloride channels. *Hum. Mol. Genet.* 3:547–552.

Vanoye, C. G., and A. L. George, Jr. 2002. Functional characterization of recombinant human ClC-4 chloride channels in cultured mammalian cells. *J. Physiol. (Lond.).* 539:373–383.